

Lithium Granular Injector Operational Experience Triggering ELMs in H-Mode on DIII-D

A. Nagy, A. Bortolon, E. P. Gilson, R. Lunsford,
R. Maingi, D.K. Mansfield, A.L. Roquemore
Princeton Plasma Physics Laboratory
Princeton, New Jersey 08543-0451, USA
nagy@fusion.gat.com

C. P. Chrobak, G. L. Jackson
General Atomics
DIII-D
PO Box 85608, San Diego, California 92186-5608, USA

Abstract—An injector device to trigger frequent edge localized modes (ELMs) was developed at Princeton Plasma Physics Laboratory (PPPL) and subsequently installed and operated on DIII-D, to inject lithium spherical granules to launch into tokamak plasmas. One size granule per shot, selectable between shots, of four different spherical lithium granule sizes are available to launch horizontally into the plasma mid-plane at speeds up to 120 m/s. Pre-sorted granules are stored in a 4-chamber reservoir containing granules at various sizes, 900, 700, 500, and 300 micron. A manually controlled gating device opens the subject reservoir compartment channeling granules to a piezo crystal with a central aperture. The disk is then electrically vibrated at its resonant frequency causing granules to fall through the aperture into a vertical tube that terminates slightly above a rotating impeller strike zone. The variable speed rotating impeller, hits the granules through an aperture gated drift tube into the plasma. The 44 cm vertical drop imparts sufficient vertical speed to the granules to reach to the impeller center. A high-speed camera records granule/impeller interaction events to provide the injection count. Another on-axis high-speed camera records the plasma edge ablation events. Impeller speed is monitored via a photodiode using an external illumination system. Initial operations injected granules at frequencies up to 120 Hz (900 micron) and >600 Hz (300 micron). ELM triggering efficiency approached 100% for 700 and 900 micron in ELMI H-mode plasmas. The injector can be used to inject other materials e.g. boron, tungsten, carbon, etc. The system and planned upgrades are discussed.

Keywords—Lithium; granular; injector; piezo; injection

I. INTRODUCTION

Naturally occurring, periodic, relaxations of the plasma edge called Edge Localized Modes (ELM), characteristic of the H-mode confinement of tokamak plasmas, are likely to cause unacceptable damage to wall components in next-step tokamak fusion devices [1]. Present day projections estimate that safe operation in ITER would require a 20-50X reduction to the peak heat flux deposited on the divertor tiles during a spontaneous ELM event [2]. This motivates the development of techniques to reliably suppress ELMs or mitigate their detrimental effects. Experimental demonstration of mitigation has been obtained by actively inducing ELMs at frequencies

much larger than the natural ELM frequency [3], effectively reducing of the amount of energy per ELM lost by the plasma and conveyed onto the divertor tiles. While reliable and effective ELM pacing has been achieved by injection of deuterium pellets [4], concern is arising about the amount of deuterium required to maintain a robust, high frequency ELM pacing in ITER, where the total fuel throughput in the vessel is limited by the capacity of pumping and tritium processing systems [5]. In that respect, the use of non-fuel pellets, e.g. low Z non-recycling elements such as Li or Be, would alleviate the load to the gas post-processing systems, and at the same time decouple ELM pacing from plasma fueling. A simple prototype device capable of injecting Lithium granules at velocities up to 100 m/s was shown to trigger ELMs in the EAST tokamak [6]. Building on that experience, an upgraded version of the Lithium Granule Injector (LGI) was recently installed on DIII-D, to study pacing efficiency dependence on granule size and velocity, and characterize LGI induced ELMs.

This paper discusses in detail the engineering aspects of the LGI project on DIII-D (design, construction, implementation on the DIII-D device, commissioning, operation and decommissioning), including preliminary results on the ELM pacing performance.

II. TECHNICAL DESCRIPTION

The LGI installed at DIII-D (Fig. 1) consists of several sections, 1. A selectable four compartment storage reservoir mounted above a piezoelectric metering disk, (granules are loaded prior to operations through the reservoir top flange), 2. A rotating impeller, with 2 paddles, (up to 10,000 rpm), that hits dropped granules into the plasma edge through a vacuum valve shield drift tube, 3. A vacuum system with low base pressure ~ 1.33 mPa, and 4. Diagnostics for measuring granule injection rate, impeller speed, and plasma ablation. The following sections describe each of these sections. See Fig. 2 for the configuration.

A. Reservoir Design

The 304 stainless steel reservoir is brazed out of discrete parts that include a solid axial shaft chamber selector held by

This work was supported by the U.S. Department of Energy under Contracts DE-AC02-09C11466 and DE-FC02-04ER54698.

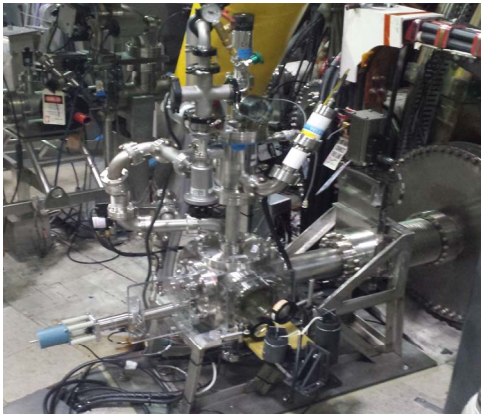


Fig. 1. Lithium Granular Injector installed on DIII-D.

Vespe[®]l bushings. At the bottom of the selector is a vertical groove, with a cut out groove (“gate”) that when aligned with a hole at the compartment bottom, guides granules to the top of the piezo disk. The selector shaft is turned by a manually operated rotary feed-through at the top vacuum flange. A piezo disk (PZD) throttles granules located on top of it via vibrations into a central hole (3 mm diameter) that is mounted to the underside of the reservoir via an electrical insulating ring made out of PEEK (polyether ether ketone). PZD wiring, attached to the disk by two annular rings (one on each side) is routed through a side electrical feed-through. The PZD is held against two concentric Viton o-rings embedded in the bottom of the reservoir; one on the PZD outer edge and one at the anti-nodal point at $\frac{1}{2}$ the diameter. A very light torque (0.011 N-m) holds the disk to the o-rings allowing it to vibrate at its resonant frequency of 2250 Hz. The PZD is centered over a 4 mm ID tube with a 1 mm gap to allow clearance for PZD movement. [7] The 0.434 m length tube exit is 1 mm above the impeller strike zone and has a large diameter robust fitting on the end that provides a broad camera viewing target. See Fig. 2 for configuration.

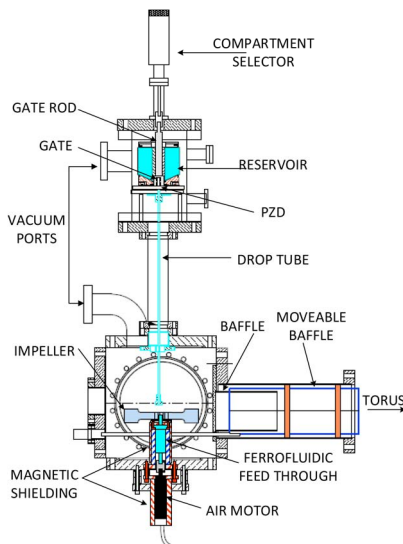


Fig. 2. LGI Elevation

B. Impeller

The impeller provides the force to strike the granules horizontally into the plasma outer edge. It is made from PEEK and coated with nickel ~ 0.010 mm thick to reduce electrostatic charge buildup. It is attached via Morse taper, with an axial screw, at the end of the ferrofluidic feed-through shaft mounted inside a magnetic shield.

The magnetic shield reduces the ambient machine field of 800 gauss to below the maximum allowable feed through field of 100 gauss. The feed through maximum speed is 10,000 rpm. An air motor (24,000 rpm max.) is coupled to the feed through air side shaft (6.35 mm dia.) via a formed bellows coupling. The 110 psig drive air is filtered and throttled through a current driven pressure control valve. [8]

C. Vacuum System

An Agilent turbo vacuum system (pumping speed 77 L/s N₂) pumps through two parallel ducts, one connected to the reservoir zone, and the other to the impeller zone to improve conductance. A fine mesh screen ~ 100 μ m covers the impeller zone port to prevent fine Lithium particles from entering the turbo duct. The base pressure in this 15 liter volume system while closed off from the main torus is ~ 4.0 mPa after 2 weeks under vacuum. The slow base pressure evolution is due to a restriction on baking, due to Lithium thermal operational limits, and the hydrocarbon materials used for electrical insulation and the impeller. A slight pressure rise is observed at the impeller daily start-up and is suspected to originate from adhered gas desorbed during the 10,000 rpm initial impeller rotation; subsequent leak checks were $< 1.6E-12$ Pa m³/s N₂ leak rate. Argon is used to vent the LGI to prevent Lithium oxidation during granule loading and unloading, and for removal from the torus.

D. Torus Interface Valve (TIV) Shield

A smaller diameter concentric baffle tube, mounted inside the front spool tube, is moved axially via servo motor through the open TIV to prevent Lithium from jamming the valve or depositing on the valve sealing surfaces. Micro-switches interlock the TIV with the shield position, preventing inadvertent TIV/shield collision. In addition the TIV close pressure is interlocked to not pressurize/close in the event of an electrical power outage.

E. Diagnostics

The LGI was equipped with a set of diagnostics to both monitor the operation and document the performance. A fast camera (Phantom 7.3, from Vision Research), installed on the side of the LGI body, was used to capture the impeller-granule impact region: acquisitions of 100x300 pixel images at 20 kHz frame rate accurately resolved the moving granules falling out of the guide tube, for determination of the impact event timing. Two illumination lights, each comprising a halogen source with a focusing lens, provided adequate illumination of the impeller impact zone, Fig. 3a. Image processing tools were applied off-line, to recover several operational quantities as a function of time, such as: 1) impeller rotation frequency, 2) the granule drop rates, 3) granule diameter (Fig. 3b), 4) number of

granules per hit, 5) injection time, and 6) injection frequency. The distribution of the inverse of inter-injection periods can be used to visualize the spectrum of injection frequency, as shown in Fig. 3c for an experiment with 250 Hz impeller rotation frequency.

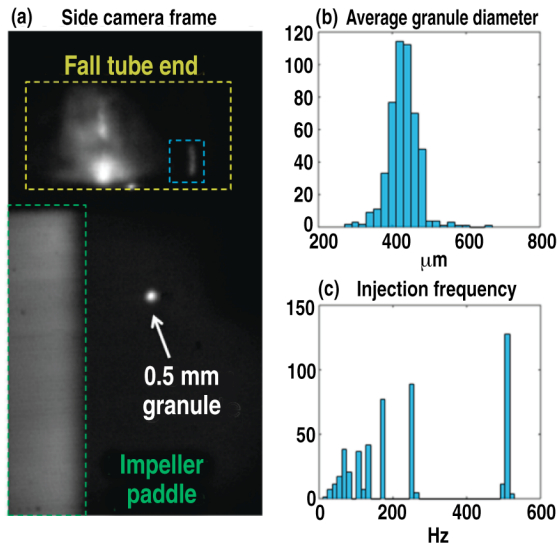


Fig. 3. (a) Fast camera image-capturing the fall of a 0.5 mm diameter granule before impeller hit (left). Image post-processing techniques are used to compute the distribution of the size of injected granules (b) and the spectrum of injection frequencies (c).

By monitoring the increase of LGI internal background light due to pellet/plasma ablation light coming back through the injection tube, a time history of the sequence of pellet ablation events could be obtained. This information can be used to discriminate actual injections into plasma from errant strikes or “foul balls”, and determine an injection efficiency (number of granules ablated/number of granules dropped), which over these experiments was $\sim 85\%$ or better. In addition, by cross-correlating the time histories of granule hits and ablation events, an estimate of the granule time of flight is derived, and consequently the granule velocity. Although granule velocity up to 110 m/s was routinely attained, this was much lower than the nominal velocity expected for elastic impacts, indicating that the Li-impeller hit is deeply inelastic, as expected from the softness of Lithium. These techniques-correlating the ablation history with other ELM behavior monitors- quantifies the ability of the LGI to trigger ELMs.

A valuable real-time impeller rotation frequency was available in the control room, obtained from the periodic light signal from a photodiode. A fast color camera (Miro II, <http://www.visionresearch.com>) was used to observe the plasma edge from a window located on the back of the LGI body, providing a radial view of the ablation region through the LGI injection tube. Color acquisitions at frame rates up to 40 kHz, were able to capture the dynamics of the granule ablation/penetration, characterized by the expansion of a field aligned cloud of ablated material (Fig. 4). The images are dominated by the green light from line emission at 548 nm, from the singly ionized Li II.

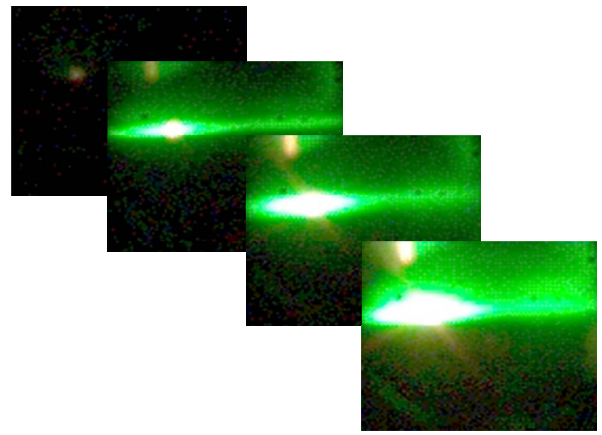


Fig. 4. Sequence of images captured by color camera, view down axis of injection tube, showing the ablation of a 0.5 mm granule. Frames are separated by 50 μ s intervals.

III. PRE-OPERATIONAL TESTS

The LGI was assembled and calibrated/tested in the lab initially using polyethylene beads for operational readiness. The beads worked well in the dropper but shattered when hit by the impeller, requiring an extended cleanup. Calibration with Lithium was subsequently performed with a target made from aluminum foil stuck to a vacuum window, using vacuum grease, located at the torus end of the flight tube. The granule drop is ~ 1.0 degree, nominally leaving the LGI injector tube 12.0 mm below mid-plane as shown in Fig. 5. An aperture masks the baffle tube entrance to provide only a line of sight path from the impeller strike zone to the vessel. (Fig. 6) Tests with 0.3 mm and 0.5 mm granules demonstrated injection rates ~ 600 -800 granules per second at piezo excitation of ~ 0.5 V peak-peak, and the 0.7 mm – 0.9 mm were 100-150/s at 40 V peak-peak PZD excitation. The trajectory drop angle is approximately 1° from horizontal reaching plasma 1.6m away. View ports were covered (60 mesh SS screen) for protection from the lithium granules and the 110 GHz high power ECH that occasionally reflects back into ports from over dense plasma. The viewing window had a 6 mm thick quartz window in addition to the mesh for protection.

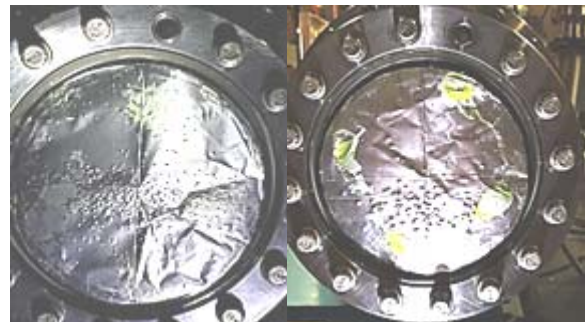


Fig. 5. Targets showing scatter of granules at the vessel flange entry point, 0.3 mm on left and 0.9 mm on right.

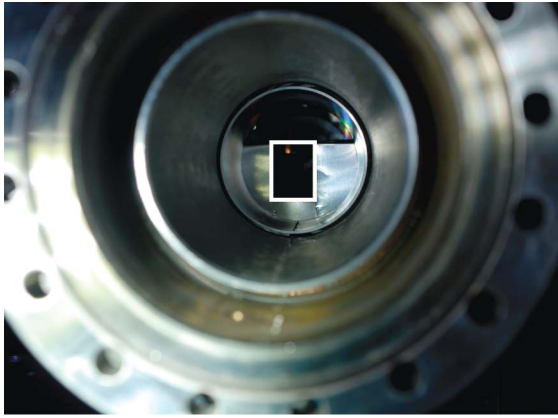


Fig. 6. The white rectangle outlines the aperture, looking from the vessel end, the semi-circle above it is a quartz glass window to observe ablations.

IV. VESSEL INSTALLATION

The LGI spool tube is centered on a radial line at the vessel mid-plane via a 0.153 m diameter bellows and TIV. A DC break was not used in order to get as close to the vessel as possible. DC electrical isolation (5kV minimum) between the LGI and external equipment is provided by discrete vacuum ceramic breaks and structural electrical insulation (G-10 sheets). Two fast cameras are used to observe granule/impeller impacts (side view) and plasma ablation events through the flight tube (axial view).

V. PRE-RUN PROCEDURES

Granules are loaded into the reservoir while the LGI is attached to the vessel by venting the LGI with Argon and keeping the purge gas flowing. The reservoir top is removed; granules loaded, and top reinstalled, and then vacuum is restored. Daily pre-run calibration of the PZD voltage versus drop rate (using ~200-300 granules in 4 shots), was performed to establish the PZD calibration for that day (e.g. Fig. 7). The air motor was oiled, and a warm-up run of the air motor/ferrofluidic feed-through tested.

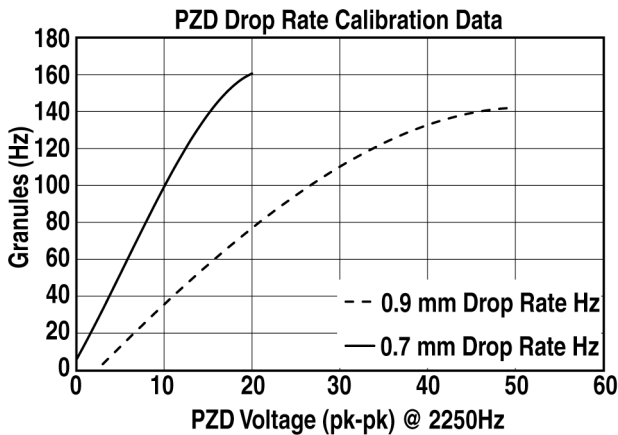


Fig. 7. showing the larger drop rate of the smaller 0.7 mm compared with the larger 0.9mm granules.

VI. LGI EXPERIMENTAL OPERATIONS

The TIV shield is inserted at the beginning of the run and left open to the torus throughout the run, including inter-shot Helium glow discharge cleaning sequences. No adverse effects were observed on either the LGI or vessel conditions. The air motor was run/warmed up during the shot cycle; 30 sec. prior to the shot start to establish a stable impeller frequency response. The PZD voltage amplitude, timing, and plasma interlock are operated through Plasma Control System programming; the impeller speed, timing, and shield position are controlled by the vacuum PLC. Granules were launched successfully triggering ELMs from the initial plasma shots during the first day of operations. LGI injections were successful in approximately 30 shots during the initial 2 day run period. A couple of shots had misfires, discussed in the next section, that were associated with using the larger granules. The 0.3 and 0.5 mm injected granules at ~600/s caused disruptions.

VII. OPERATIONAL CHALLENGES

Trouble with granule flow was caused by granules bridging over the feed passage during the flow period; these are called bridge instabilities. The 0.7 mm and 0.9 mm granules would stick above the PZD during a shot, interrupting the flow to the PZD causing blank zones in the injected granule series, or causing a whole shot misfire. This was successfully avoided by manually striking the reservoir zone, after each shot, to shake the granules loose. It was found subsequently during a steady state drop test with a PZD voltage of 20 V pk-pk that the 0.9 mm granule flow would stop after ~3 seconds and the 0.7 mm granules after ~4 seconds. A second issue was associated with drift in the air motor speed, which is thought due to ferrofluidic feed-through warm-up. The speed was inconsistent, requiring manual adjustment of the air feed pressure setting, even though extensively calibrated in the lab. This behavior became more consistent after many shots and oiling of the air motor, and is believed to have been caused by improper oiling during air motor break-in.

VIII. PRELIMINARY RESULTS

The LGI was tested in ELMy H-modes characterized by an electron density of $n_e=4\text{-}6 \times 10^{19} \text{ m}^{-3}$ and temperature $T_e=600\text{-}700 \text{ keV}$, at the top of the plasma pedestal (2-3 cm inside the plasma boundary). Granules with a nominal diameter 0.3, 0.5, 0.7 and 0.9 mm were tested in a shot-by-shot fashion, with injection speeds of 50-120 m/s and time averaged injection rates up to 100 Hz for 0.9 mm granules and up to 700 Hz for 0.3mm granules. Robust ELM pacing was documented for long time windows (up to 3.5 s), with triggering efficiency close to 100% obtained with 0.7 and 0.9 mm granules. To exemplify the LGI performance, figure 8(a) compares the time evolution of the D_α line emission from the divertor region with the ablation light detected in the fast-camera images, for a plasma discharge with 0.9 mm granules injected at 120 m/s, at an average frequency of 95 Hz. A consistent one-to-one correspondence between spikes in the D_α signal (indicative of ELMs) and spikes in the detected ablation light is observed, demonstrating robust ELM pacing at frequencies 3-5 times the

natural ELM frequency (20-30 Hz). Moreover, as a result of the fluctuations of the injection frequency, transient phases of ELM pacing at frequencies above 200 Hz were observed.

Detailed analysis of the acquired dataset is in progress and will be the subject of a future publication [9]. In general, LGI high frequency pacing appeared to be compatible with high plasma performance, both in terms of global confinement and pedestal characteristics.

IX. FINDINGS AFTER OPERATIONS

Upon LGI removal from the vessel it was disassembled and cleaned. Lithium granules, pieces, and dust, were found scattered throughout the LGI. The TIV's operation or seal was not compromised with some small granules discovered in the valve body bottom. There was however lithium dust and small pieces inside the shield tube, Conflat® seal zone, and TIV housing bottom shown in Fig. 9.

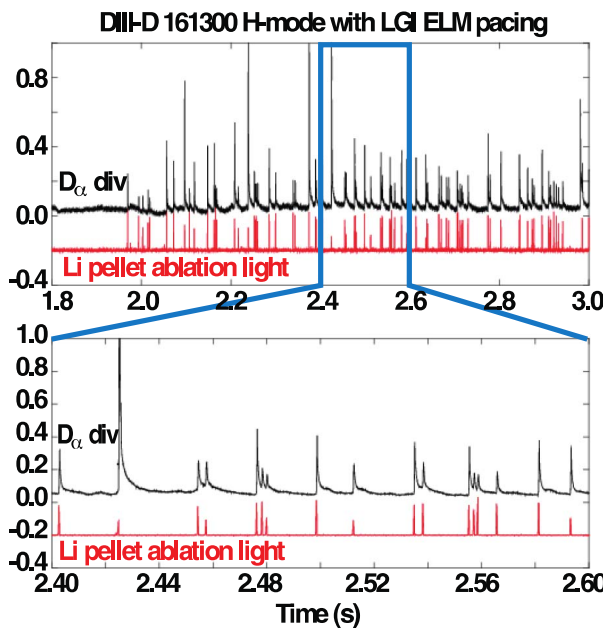


Fig. 8. (a) Spikes in the $D\alpha$ emission from the divertor indicative of ELM activity (black) correlate with light bursts associated with granule ablation (red).

Accumulations of dust were found in all Conflat® flange bottoms in the gap between flanges against the copper Conflat® seal. No copper corrosion was found due to Lithium contact on any of the surfaces. Surprisingly few granules were found in the bottom of the bellows and vessel port nozzle downstream of the TIV. Granules were also found in ports toroidally adjacent to the LGI port and associated with an inadvertent launching of granules during a mechanical impulse with impeller testing between shots with the TIV open. The LGI was taken apart to install a larger PZD with a 3 mm center hole after the initial run using a PZD with a 2.5mm hole. This successfully increased the large granule injection rate from ~100 to 150/s. The reservoir was clogged at the end of the first run and disassembled and inspected for root causes. Granules were found stuck in the “gateway” and on the PZD which appeared due to a liquid that stained the PZD (Fig. 9). The

PZD oil stain evaporated after 1 day air exposure, and appeared to be mineral oil residue from the manufacture of the 0.7 and 0.9 mm granules. This process included a final granule wash with hexane, and drying them in a vacuum system with a mass spectrum until the oil peaks were at noise level. The granules were recovered from the reservoir and reused for the next run without washing; the PZD and gate were found to remain clean after the second run (Fig. 10).



Fig. 9. Lithium granules (gray spheres) on the bottom of the injection baffle, and TIV copper seal and valve bottom.

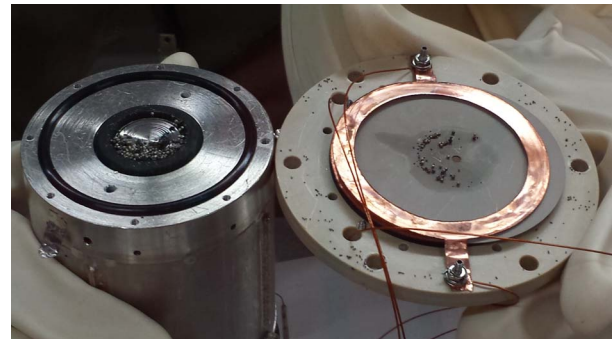


Fig. 10. Reservoir bottom on left and PZD on right, both with granules of various diameters stuck on the drop zone surfaces. The liquid stain on the PZD was suspected to be mineral oil from granules production.

An additional finding was the gate rod annular accumulation of Lithium thought due to small granules being extruded into this gap. The radial gap on the first unit was ~0.2 mm, which needed increasing amounts of torque to rotate after few rotations, leading to the prospect of seizure. The second reservoir radial gap is much tighter at .025 mm, and the rotational torque of the gate rod remained more constant enabling easier rotation without fear of seizure. Fig. 12 shows that the tighter gap had significantly less Lithium annular accumulation in the gate rod section.

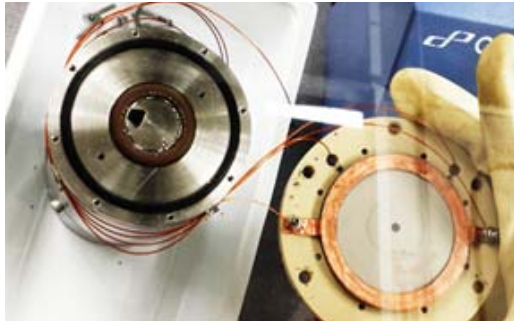


Fig. 11. PZD inspection after second run-no granule accumulation on surfaces or in “gateway.”

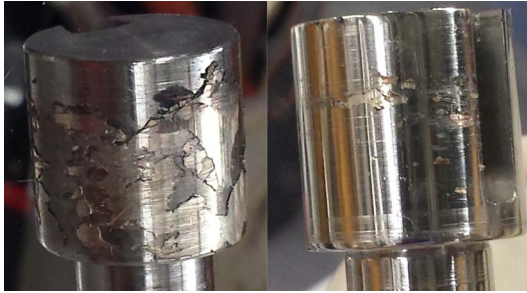


Fig. 12. (Left) Gate rod to housing has a 0.2 mm radial clearance and right is .025 mm clearance. The larger clearance filled with Lithium and inhibited easy rotary motion.

X. CONCLUSIONS/FUTURE UPGRADES

To prevent the bridge instabilities described above in the dropper portion of the LGI, gate channel stirrers made of a flat piezoelectric sheet will be fitted inside each reservoir compartment. These will be driven to vibrate at their resonant frequency to keep the granules moving fluidly. An electric motor with speed feedback will be installed within the magnetic shield to stabilize impeller rotation speed. Fast cameras will be eliminated and their function replaced by photodiodes to record ablation events and granule drop frequency. Regulation of the injection frequency is the largest challenge, due to the granule size and Lithium’s soft nature; solutions are being explored. Additionally, other materials for

impurity injection down to the single granule per shot level are being considered e.g. boron carbide, carbon, and tungsten. Initial lab tests with boron carbide and vitreous carbon have been successful.

In conclusion, the two runs on DIII-D were highly successful to demonstrate proof of principle to trigger ELMs using this injection device and method. Once improved regulation of the injection frequency is developed, and the bridge instability resolutions are completed, this equipment should become a regular tool in ELM physics studies.

ACKNOWLEDGMENT

Our LGI success came through many hours of work from Will D. Brown, Tom Holoman, and Tom Provost, our loyal technicians, who diligently and patiently supported this effort during its preparation, installation, and operations on DIII-D.

REFERENCES

- [1] A.W. Leonard, “Edge-localized-modes in tokamaks,” 2014 Phys. Plasma 21 090501
- [2] A. Loarte, G. Huijsmans, S. Futatani, L.R. Baylor, T.E. Evans, D.M. Orlov, et al., “Progress on the application of ELM control schemes to ITER scenarios from the non-active phase to DT operation,” 2014 Nucl. Fusion 54 033007
- [3] R. Maingi, “Enhanced confinement scenarios without large edge localized modes in tokamaks: control, performance, and extrapolability issues for ITER,” 2014 Nucl. Fusion 54 114016
- [4] L.R. Baylor, N. Commaux, T.C. Jernigan, N.H. Brooks, S.K. Combs, T.E. Evans, et al., “Reduction of Edge-Localized Mode Intensity Using High-Repetition-Rate Pellet Injection in Tokamak H-Mode Plasmas,” 2013 Phys. Rev. Lett. 110 245001
- [5] A.S. Kukushkin, A.R. Polevoia, H.D. Pacharb, G.W. Pacherc, R.A. Pitts, “Physics requirements on fuel throughput in ITER,” 2011 *J. Nucl. Mater.* 415 S497
- [6] D.K. Mansfield, A.L. Roquemore, T. Carroll, Z. Sun, J.S. Hu, L. Zhang, et al., “First observations of ELM triggering by injected lithium granules in EAST,” 2013 Nucl. Fusion 53 113023
- [7] D.K. Mansfield, A.L. Roquemore, H. Schneider, J. Timberlake, H. Kugel, M.G. Bell, et al., “A simple apparatus for the injection of lithium aerosol into the scrape-off layer of fusion research devices,” 2010 Fusion Eng. and Design 85 890
- [8] A.L. Roquemore, B. John, F. Friesen, K. Hartzfeld, D.K. Mansfield, 2011 Fusion Eng. and Design 86 1355
- [9] A. Bortolon, et al. Nucl. Fusion, to be submitted.